



Since January 2020 Elsevier has created a COVID-19 resource centre with free information in English and Mandarin on the novel coronavirus COVID-19. The COVID-19 resource centre is hosted on Elsevier Connect, the company's public news and information website.

Elsevier hereby grants permission to make all its COVID-19-related research that is available on the COVID-19 resource centre - including this research content - immediately available in PubMed Central and other publicly funded repositories, such as the WHO COVID database with rights for unrestricted research re-use and analyses in any form or by any means with acknowledgement of the original source. These permissions are granted for free by Elsevier for as long as the COVID-19 resource centre remains active.



Up-regulated 60S ribosomal protein L18 in PEDV N protein-induced S-phase arrested host cells promotes viral replication

Qinghe Zhu^{a,1}, Mingjun Su^{a,c,1}, Shan Wei^{a,1}, Da Shi^b, Lu Li^a, Jun Wang^a, Haibo Sun^a, Meijiao Wang^a, Chunqiu Li^a, Donghua Guo^a, Dongbo Sun^{a,*}

^a College of Animal Science and Veterinary Medicine, Heilongjiang Bayi Agricultural University, No. 5 Xinfeng Road, Sartu District, Daqing 163319, China

^b State Key Laboratory of Veterinary Biotechnology, Harbin Veterinary Research Institute, Chinese Academy of Agricultural Sciences, Harbin 150069, China

^c Key Laboratory of Applied Technology on Green-Eco-Healthy Animal Husbandry of Zhejiang Province, Zhejiang Provincial Engineering Research Center for Animal Health Diagnostics and Advanced Technology, Zhejiang International Science and Technology Cooperation Base for Veterinary Medicine and Health Management, China-Australia Joint Laboratory for Animal Health Big Data Analytics, College of Animal Science and Technology and College of Veterinary Medicine of Zhejiang A&F University, 666 Wusu Street, Lin'an District, Hangzhou, Zhejiang 311300, China

ARTICLE INFO

Keywords:

coronavirus
PEDV
Cell cycle arrest
Ribosomal protein L18
Virus replication

ABSTRACT

Coronavirus subverts the host cell cycle to create a favorable cellular environment that enhances viral replication in host cells. Previous studies have revealed that nucleocapsid (N) protein of the coronavirus porcine epidemic diarrhea virus (PEDV) interacts with p53 to induce cell cycle arrest in S-phase and promotes viral replication. However, the mechanism by which viral replication is increased in the PEDV N protein-induced S-phase arrested cells remains unknown. In the current study, the protein expression profiles of PEDV N protein-induced S-phase arrested Vero E6 cells and thymidine-induced S-phase arrested Vero E6 cells were characterized by tandem mass tag-labeled quantitative proteomic technology. The effect of differentially expressed proteins (DEPs) on PEDV replication was investigated. The results indicated that a total of 5709 proteins, including 20,560 peptides, were identified, of which 58 and 26 DEPs were identified in the PEDV N group and thymidine group, respectively ($P < 0.05$; ratio ≥ 1.2 or ≤ 0.8). The unique DEPs identified in the PEDV N group were mainly involved in DNA replication, transcription, and protein synthesis, of which 60S ribosomal protein L18 (RPL18) exhibited significantly up-regulated expression in the PEDV N protein-induced S-phase arrested Vero E6/IPEC-J2 cells and PEDV-infected IPEC-J2 cells ($P < 0.05$). Further studies revealed that the RPL18 protein could significantly enhance PEDV replication ($P < 0.05$). Our findings reveal a mechanism regarding increased viral replication when the PEDV N protein-induced host cells are in S-phase arrest. These data also provide evidence that PEDV maintains its own replication by utilizing protein synthesis-associated ribosomal proteins.

1. Introduction

Coronaviruses are a class of viruses with capsids and linear single-stranded positive-stranded RNA genomes that are widespread in nature and can infect humans, mammals, and birds (Shi, 2021; Wang et al., 2022). Over the past 20 years, frequent outbreaks of human and animal coronaviruses have occurred worldwide, resulting in serious disaster to human society and serious challenges to public health safety and animal health (Cui et al., 2019; Li et al., 2022). Porcine epidemic diarrhea virus (PEDV) is an enveloped, single-stranded, positive-sense RNA virus that belongs to the order *Nidovirales*, family *Coronaviridae*, and genus

Alphacoronavirus (Su et al., 2020b). PEDV causes severe watery diarrhea, vomiting, dehydration, and a mortality rate of up to 100% in suckling piglets. Vaccination represents the preferred strategy for the prevention and control of PEDV (Sun et al., 2016); however, PEDV still occurs frequently due to rapid virus mutation, strain varieties, and delayed vaccine updates, which has led to tremendous economic losses in the global swine industry (Gerds and Zakhartchouk, 2017; Wang et al., 2019). Therefore, the study of the PEDV infection mechanism is required for designing antiviral strategies.

Viruses are specific live intracellular parasites that must rely on host cell resources to complete the virus's own replication (Su et al., 2020a).

* Corresponding author.

E-mail address: dongbosun@126.com (D. Sun).

¹ These authors contributed equally to this work.

A common mechanism used by viruses to establish an infection is by altering biological processes such as the host cell cycle and acquiring factors associated with their own replication (Bagga and Bouchard, 2014; Nascimento et al., 2012). A proven viral strategy is to modulate the host cell cycle to promote virus growth (Bagga and Bouchard, 2014). Various coronaviruses have evolved multiple strategies to regulate the host cell cycle according to the characteristics of their own replication. Moreover, they can induce host cell cycle arrest during the S-phase or G1/G2-phase to create a favorable cellular environment for viral replication (Bouhaddou et al., 2020; Yuan et al., 2007). An accumulated number of studies have gradually revealed the molecular mechanism regarding the coronavirus-induced host cell cycle arrest. Coronaviruses manipulate the cell cycle by regulating the Cyclin-CDK complex, p53-dependent pathway, the coronavirus nucleocapsid (N) protein, and the direct interaction with host cell cycle-associated proteins (Ding et al., 2013; Ding et al., 2014). Our previous studies reveal that the PEDV N protein interacts with p53 to activate the p53-DREAM pathway, and subsequently induces cell cycle S-phase arrest to create a favorable environment for viral replication (Su et al., 2021). At present, although the mechanism of coronavirus-mediated host cell cycle arrest has been widely studied, the mechanistic details regarding increased viral replication in the coronavirus-induced host cell cycle arrested cells remain unclear.

In our study, a large-scale proteomic investigation based on tandem mass tag (TMT) combined with liquid chromatography-tandem mass spectrometry (LC-MS/MS) was conducted to comprehensively reveal the protein expression profile of the PEDV N protein-induced S-phase arrested Vero E6 cells (PEDV N group) and thymidine-induced S-phase arrested Vero E6 cells (thymidine group). The unique differentially expressed proteins (DEPs) of the PEDV N protein-induced S-phase arrested Vero E6 cells were obtained through a comparison with the DEPs identified in the thymidine-induced S-phase arrested Vero E6 cells. The Gene Ontology (GO) category, Kyoto Encyclopedia of Genes and Genomes (KEGG) annotation, and protein-protein interaction (PPI) network analysis revealed the highlighted 60S ribosomal protein L18 (RPL18), which is potentially responsible for the mechanism regarding enhancing viral replication in host cells when the PEDV N protein interacts with p53 to induce host cell cycle arrest in S-phase. Our study reveals a novel mechanism regarding increased viral replication by which the PEDV N protein induces host cell S-phase arrest. These data also provide a reference for the mechanism by which SARS-CoV-2 and other coronaviruses regulate the host cell cycle and design antiviral drugs based on this mechanism.

2. Materials and methods

2.1. Virus, cells, antibody, and reagents

The PEDV strain, CV777 (GenBank accession no. KT323979), was kindly provided by the Division of Swine Digestive System Infectious Diseases, State Key Laboratory of Veterinary Biotechnology, Harbin Veterinary Research Institute, Chinese Academy of Agricultural Sciences. The PEDV strain, HM2017 (subgroup GII-a, GenBank accession no. MK690502), was isolated and stored in the Laboratory of Swine Infectious Diseases, College of Animal Science and Veterinary Medicine, Heilongjiang Bayi Agricultural University (Yang et al., 2020). The Vero E6 cells and porcine intestinal epithelial cells (IPEC-J2) were stored at the Laboratory of Swine Infectious Diseases, College of Animal Science and Veterinary Medicine, Heilongjiang Bayi Agricultural University. The cells were cultured in Dulbecco's modified Eagle medium (DMEM) supplemented with 10% fetal bovine serum (FBS) under a humidified atmosphere of 5% CO₂ at 37 °C. Monoclonal antibodies (mAbs) against the PEDV N protein were kindly provided by the Division of Swine Digestive System Infectious Diseases, State Key Laboratory of Veterinary Biotechnology, Harbin Veterinary Research Institute, Chinese Academy of Agricultural Sciences. A polyclonal antibody against RPL18

(17029-1-AP) was purchased from Proteintech Group. The GAPDH antibody (G8795) and GFP antibody (AG281) were obtained from Sigma-Aldrich (St. Louis, MO, USA) and Beyotime Biotechnology (China), respectively.

2.2. Plasmids

The N gene was amplified using RT-PCR (Primer: PEDV N-F: 5'-GCC TCG AGT ATG GCT TCT GTC AGC TTT CAG GAT C-3'; PEDV N-R: 5'-GCG GTA CCT TAA TTT CCT GTA TCG AAG ATC TCG T-3') from the PEDV CV777 strain (GenBank accession no. KT323979) and cloned into the vectors pAcGFP1-C1 (with *Xho*I and *Kpn*I restriction enzymes) and pCMV-Myc (with the *Sa*I and *Kpn*I restriction enzymes), respectively. The plasmids were termed pAcGFP1-C1-N and pCMV-Myc-N. A pair of specific primers (RPL18-F: 5'-GAA TTC TAT GGG AGT TGA CAT C-3'; RPL18-R: 5'-GGA TCC TTA GTT TTT GTA GCC GCG G-3') were designed according to the nucleotide sequences of the RPL-18 gene (GenBank accession no. XM_021094700.1). The RPL18 gene was amplified from IPEC-J2 cells using specific primers. The amplified RPL18 gene was cloned into the eukaryotic expression vector pAcGFP1-C1 with the *Xho*I and *Kpn*I restriction enzymes. The recombinant plasmids of the RPL18 gene were termed pAcGFP1-C1-RPL18.

2.3. Quantitative proteomics sample preparation

To prepare quantitative proteomics samples of PEDV N protein-induced S-phase arrested Vero E6 cells and thymidine-induced S-phase arrested Vero E6 cells, the Vero E6 cells were used for the overexpression of PEDV N protein with GFP tag (GFP-N) and synchronized during S-phase, respectively. Briefly, Vero E6 cells were seeded into six well plates and transfected using the pAcGFP1-C1-N (GFP-N) and pAcGFP1-C1 empty vector (GFP) plasmids (4.5 mg per well) using Lipofectamine 3000 transfection reagent (L3000008; Invitrogen Life Technologies) according to the manufacturer's instructions. At 6 h post-transfection (hpt), the transfection mixture was replaced with complete growth medium and incubated for an additional 18 h before being used in assays. Vero E6 cells were synchronized by incubating cells with an excess of 0.85 mM thymidine (T1895; Sigma) for 18 h. Cells were washed two times with 1 × PBS and incubated in DMEM-FBS without thymidine for 8 h, followed by a second exposure to 0.85 mM thymidine. After 16 h, the cells were collected for further assays. All cell samples were analyzed by flow cytometry prior to a proteomic analysis. For all proteomics experiments, three biological replicates were performed for each sample, including the control sample.

2.4. Cell cycle assay

Vero E6 cells in which GFP-N was expressed were collected and fixed in 70% cold ethanol overnight at 4°C. After washing with PBS (pH 7.4), the cells were resuspended and strained with propidium iodide (PI, 50 mg/mL) and RNase A (100 mg/mL) (550825; BD Biosciences) for 15 min at room temperature in the dark. Cell cycle distribution was performed using an Accuri C6 flow cytometer (BD Biosciences). Data were analyzed using ModFit LT 5.0 (Verity Software House).

2.5. Tandem mass tag (TMT)-labeled quantitative proteomic analysis

Tandem mass tag (TMT)-labeled quantitative proteomic analysis of the PEDV N/thymidine-induced S-phase arrested Vero E6 cells was performed in accordance with Fig. 1.

2.5.1. Protein extraction

Twelve samples, including three samples of PEDV N protein-induced S-phase arrested Vero E6 cells, three GFP control samples, three samples of thymidine-induced S-phase arrested Vero E6 cells, and three DMSO control samples were homogenized in lysis buffer (4% SDS, 1 mM DTT,

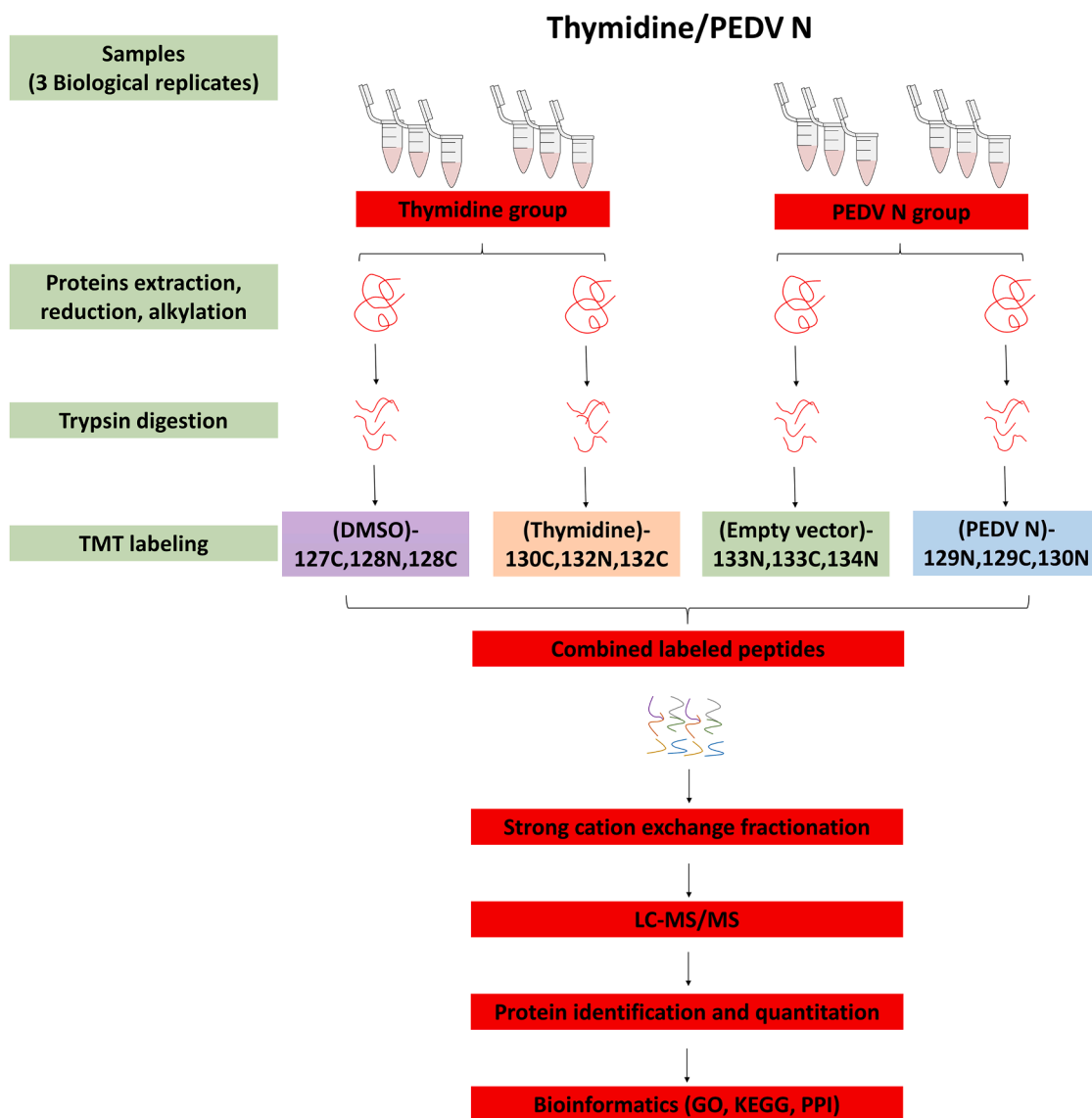


Fig. 1. Schematic flow diagram of tandem mass tag (TMT)-labeled quantitative proteomic analysis of the PEDV N/thymidine-induced S-phase arrested Vero E6 cells.

150 mM Tris-HCl pH 8.0, protease inhibitor). After a 3 min incubation in boiling water, the homogenates were sonicated on ice. Next, the crude extract was incubated in boiling water and clarified by centrifugation for 10 min at $16,000 \times g$ and 25°C . The protein content was determined using BCA protein assay reagent (Beyotime). The supernatants were stored at -80°C until further use.

2.5.2. Protein digestion and TMT labeling

Protein digestion was performed according to the FASP procedure described by Wisniewski et al. (2009), and the resulting peptide mixture was labeled with 16-plex TMT reagent according to the manufacturer's instructions (Applied Biosystems). Briefly, 200 μg of protein from each sample was incorporated into 30 μL SDT buffer (4% SDS, 100 mM DTT, 150 mM Tris-HCl pH 8.0). The detergent, DTT and other low-molecular-weight components were removed using UA buffer (8 M Urea, 150 mM Tris-HCl pH 8.0) by repeated ultrafiltration (Pall units, 10 kDa). Next, 100 μL 0.05 M iodoacetamide in UA buffer was added to block reduced cysteine residues and the samples were incubated for 20 min in the dark. The filters were washed three times with 100 μL UA buffer and twice with 100 μL DS buffer (50 mM triethylammoniumbicarbonate at pH 8.5). Finally, the protein suspensions were digested with 2 μg trypsin (Promega) in 40 μL DS buffer overnight at 37°C , and

the resulting peptides were collected as a filtrate. The peptide content was estimated by UV light spectral density at 280 nm using an extinction coefficient of 1.1 of a 0.1% (g/L) solution calculated based on the frequency of tryptophan and tyrosine in vertebrate proteins.

For labeling, TMT reagent was dissolved in 70 μL of ethanol and added to the respective peptide mixture. The samples were labeled as (DMSO)-127C,128N,128C, (Thymidine)-130C,132N,132C, (Empty vector)-133N,133C,134N, (PEDV N)-129N,129C,130N, multiplexed, and vacuum dried.

2.5.3. Peptide fractionation with strong cation exchange (SCX) chromatography

TMT-labeled peptides were fractionated by SCX chromatography using the AKTA Purifier system (GE Healthcare). The dried peptide mixture was reconstituted and acidified with 2 mL buffer A (10 mM KH_2PO_4 in 25% of ACN, pH 2.7) and loaded onto a PolySULFOETHYL 4.6 \times 100 mm column (5 μm , 200 \AA , PolyLC Inc, Maryland, USA). The peptides were eluted at a flow rate of 1 mL/min with a gradient of 0%–10% buffer B (500 mM KCl, 10 mM KH_2PO_4 in 25% of ACN, pH 2.7) for 2 min, 10%–20% buffer B for 25 min, 20%–45% buffer B for 5 min, and 50%–100% buffer B for 5 min. The elution was monitored at an absorbance of 214 nm and fractions were collected every 1 min. The collected

fractions (about 30 fractions) were finally combined into 10 pools and desalted on C18 Cartridges (Empore™ SPE Cartridges C18 (standard density), bed I.D. 7 mm, volume 3 mL, Sigma). Each fraction was concentrated by vacuum centrifugation and reconstituted in 40 µL of 0.1% (v/v) trifluoroacetic acid. All samples were stored at -80 °C until LC-MS/MS analysis.

2.5.4. Liquid chromatography (LC)-electrospray ionization (ESI) tandem MS (MS/MS) analysis by orbitrap fusion

Experiments were performed on a Q Exactive HF-X orbitrap mass spectrometer coupled to Easy nLC (Thermo Fisher Scientific), and 5 µL of each fraction was injected for nanoLC-MS/MS analysis. The peptide mixture (2 µg) was loaded onto a C18-reversed phase column (15 cm-long, 75 µm inner diameter) packed in-house with RP-C18 5 µm resin in buffer A (0.1% Formic acid) and separated with a linear gradient of buffer B (80% acetonitrile and 0.1% Formic acid) at a flow rate of 250 nL/min controlled by IntelliFlow technology over 60 min. MS data was acquired using a data-dependent top20 method by dynamically selecting the most abundant precursor ions from the survey scan (300–1800 m/z) for HCD fragmentation. Determination of the target value was based on predictive Automatic Gain Control (pAGC). The dynamic exclusion duration was 60 s. The scans were obtained at the resolution of 70,000 at m/z 200 and the value of resolution for high energy collisional dissociation spectra were set at 60,000 at m/z 200 (TMT 16plex), and the width of isolation was 2 m/z. The normalized collision energy was 30 eV and the AGC Target is 200,000. The instrument was run with the peptide recognition mode enabled.

2.5.5. Sequence database searching and data analysis

MS/MS spectra were searched using MASCOT engine (Matrix Science, London, UK; version 2.2) embedded into Proteome Discoverer 1.4 (Thermo Electron, San Jose, CA.) against the UniProt Chlorocebus sabaeus database (19,525 sequences, download at 20200518) and the decoy database. For protein identification, the following options were used: Peptide mass tolerance = 20 ppm, MS/MS tolerance = 0.1 Da, Enzyme = Trypsin, Missed cleavage = 2, Fixed modification: Carbamidomethyl (C), TMT16 (K), TMT16 (N-term), Variable modification: oxidation (M), and FDR ≤ 0.01.

2.5.6. Bioinformatics

The GO program Blast2GO (<https://www.blast2go.com/>) was used to annotate the DEPs to create histograms of GO annotation, including cellular components, biological processes, and molecular function. For the pathway analysis, the DEPs were mapped to the terms in the KEGG database using the KAAS program (http://www.genome.jp/kaas-bin/kaas_main).

PPI networks were analyzed using the publicly available program STRING (<http://string-db.org/>) and the minimum required interaction score was set at 0.400. STRING is a database of known and predicted protein-protein interactions. The interactions include direct (physical) and indirect (functional) associations, and are derived from four sources: the genomic context, high-throughput experiments, coexpression, and previous knowledge.

2.6. Validation of RPL18 protein expression levels

To verify the up-regulated expression of the RPL18, the PEDV N protein-induced S-phase arrested Vero E6 cells and the PEDV N protein-induced S-phase arrested IPEC-J2 cells were prepared according to the above methods (Section 2.3). The RPL18 protein of the prepared cells was subjected to detection and analysis via Western blot according to the previous protocol described by Li et al. (2019). Briefly, the total cellular proteins were extracted with RIPA lysis buffer (R0278; Sigma). The extracted proteins were then separated on a 12% sodium dodecyl sulfate-polyacrylamide gel electrophoresis (SDS-PAGE) gel and transferred to a polyvinylidene difluoride membrane. The membranes were

blocked with 5% nonfat dry milk in PBST (PBS + 0.05% Tween-20) for 2 h and incubated with the primary antibody overnight at 4 °C. After washing with 0.05% Tween-20 in PBST, the membranes were incubated with horseradish peroxidase (HRP)-conjugated secondary antibodies. After washing with 0.05% PBST, the membranes were detected with LuminataTMCrescendo Western HRP substrate (Merck KGaA, Darmstadt, Germany) using an Amersham Imager 600 (GE Healthcare, Chicago, IL, USA). The level of target protein expression was analyzed with Image J software (National Institutes of Health, Bethesda, MD, USA).

To investigate the level of RPL18 protein expression in PEDV-infected IPEC-J2 cells, the IPEC-J2 cells were incubated with PEDV strain CV777 at an MOI of 1.0 at 37 °C. The cell samples were collected at 36 hours post-infection following PEDV infection. The level of RPL18 protein expression in the PEDV-infected IPEC-J2 cells was evaluated via Western blot. Western blotting was carried out according to the above protocol.

2.7. Influence of RPL18 protein overexpression on PEDV replication

pAcGFP1-C1-RPL18 recombinant plasmids were extracted using an EndoFree Plasmid Maxi Kit (Qiagen, Hilden, Germany) and subsequently transfected into IPEC-J2 cells. Transient expression of the RPL18 gene in the IPEC-J2 cells was verified by Western blot after pAcGFP1-C1-RPL18 recombinant plasmid transfection for 24 h. IPEC-J2 cells expressing RPL18 were incubated with PEDV strain CV777 and PEDV strain HM2017 at an MOI of 1.0 at 37°C for 48 h. The viral titers of the samples were tested using the median tissue culture infective dose (TCID₅₀). Briefly, IPEC-J2 cells were seeded into a 96-well plate at a density of 10⁵ cells per well in 100 µL of medium and incubated for 48 h at 37°C under an atmosphere of 5% CO₂/95% air. The medium was removed and 100 µL of 10-fold serial dilutions of virus were added to each well. The cytopathic effect was examined every 12 h for 5 days post-inoculation. The viral titer was calculated according to the Reed and Muench method (Nemeth et al., 2018).

2.8. Effects of silenced RPL18 protein on PEDV replication

To investigate the effect of the silenced RPL18 protein on PEDV replication, small interfering RNA (siRNA) duplexes targeting the RPL18 gene (sus-17: 5'-GCC ACA AGG ACC GAA ATT-3'; sus-238: 5'-GCU GUG GUC GUA GGG ACU ATT-3'; sus-482: 5'-GCC ACA CCA AAC CCU AUG UTT-3') were synthesized, respectively. The down-regulated expression of the RPL18 protein in the PEDV-uninfected IPEC-J2 cells was identified by Western blot. IPEC-J2 cells were transfected with sus-17, sus-238, and sus-482 siRNA using Attractene Transfection Reagent (Qiagen), respectively. IPEC-J2 cells were incubated with PEDV strain CV777 and PEDV strain HM2017 at an MOI of 1.0 at 48 h following transfection with siRNAs for 24 h. The viral titers of the samples were tested using TCID₅₀ according to the above methods (Section 2.7).

2.9. Statistical analysis

Values were expressed as the mean ± standard deviation (SD). All statistical analyses were performed using GraphPad Prism 8.00 software (GraphPad Software, Inc., La Jolla, CA, USA). A one-way analysis of variance and Student's *t*-test were performed for data analysis and graph production. A probability (*P*) value of < 0.05 was considered statistically significant and *P* < 0.01 was considered to be highly significant.

3. Results

3.1. Preparation of PEDV N/thymidine-induced S-phase arrested Vero E6 cells

To obtain PEDV N protein-induced S-phase arrested cells, recombinant plasmids encoding GFP-N or GFP (empty vector) were transfected

into the Vero E6 cells. At 36 h post-transfection (hpt), Vero E6 cells were collected for an analysis of the cell cycle distribution. For the purpose of a contrast analysis, thymidine-induced S-phase arrested Vero E6 cells were generated by adding 0.85 mM of thymidine (T1895) into the growth medium of the Vero E6 cells. After a 24 h incubation with thymidine, the cell cycle distribution of the Vero E6 cells was analyzed. The flow cytometry analysis results are shown in Table S1. The Vero E6 cells were revealed to be in the S-phase when the cells were transfected with the PEDV N recombinant plasmids; the number of S-phase arrested cells in the PEDV GFP-N group (53.59%) was significantly higher than that in the GFP control group (31.99%) ($P < 0.01$, Fig. 2A). The cell cycle distribution analysis of the thymidine-treated cells indicated that 41.73% of the Vero E6 cells in the thymidine group were in the S-phase, which was significantly higher than that of the DMSO control group (21.24%) ($P < 0.01$, Fig. 2B). These data confirm that the PEDV N/thymidine-induced S-phase arrested Vero E6 cells were successfully prepared for quantitative proteomics analysis.

3.2. Protein identification and analysis of the PEDV N/thymidine-induced S-phase arrested Vero E6 cells

The protein expression profile of the PEDV N protein-induced S-phase arrested cells (PEDV N group) and the thymidine-induced S-phase arrested cells (thymidine group) was identified using TMT coupled with LC-MS/MS (Fig. 1). The identified peptides and proteins lists are presented in Tables S2 and S3. The DEPs are shown in Tables S4 and S5. A total of 5709 proteins were identified, including 20,560 peptides (Table 1). Of the 5709 proteins, 26 DEPs were identified in the thymidine group ($P < 0.05$, quantitative ratio ≥ 1.2 or ≤ 0.83), of which 15 and 11 proteins were up-regulated and down-regulated, respectively. A total of 58 DEPs were identified in the PEDV N group ($P < 0.05$, quantitative ratio ≥ 1.2 or ≤ 0.83), of which 27 and 31 proteins were up-

Table 1

The peptides and proteins identified from the PEDV N/Thymidine-induced S-phase arrest cells.

Classification		Numbers
Total peptides and proteins identified in our study	Identified peptides	20560
	Identified proteins	5709
The differentially expressed proteins between CTRL and Thymidine groups	Differentially expressed proteins	26
	Up-regulated proteins	15
	Down-regulated proteins	11
	proteins	
The differentially expressed proteins between Vector and PEDV N groups	Differentially expressed proteins	58
	Up-regulated proteins	27
	Down-regulated proteins	31
	proteins	

regulated and down-regulated, respectively. The level of change in DEP expression is shown in the volcano plot (Fig. 3A and B). The hierarchical cluster of the DEPs is presented in the heat map (Fig. 3C and D). The DEPs were subjected to an analyses of the GO and KEGG pathways (Tables S6 and S7). The 26 DEPs identified in the thymidine group were significantly enriched in 69 biological process, 30 cell components, 18 molecular functions, and 1 KEGG pathway annotation ($P < 0.05$, Fig. 4A). The 58 DEPs identified in the PEDV N group were significantly enriched in 75 biological process, 28 cell components, 10 molecular functions and 3 KEGG pathway annotations ($P < 0.05$, Fig. 4B). The significantly enriched biological processes, cell components, molecular functions, and KEGG pathway exhibited variation at the different levels between the PEDV N and thymidine groups (Fig. 4C–J).

Further analysis revealed that 10 proteins were the shared DEPs between the PEDV N and thymidine groups (Table S8). There were 13 proteins that were unique DEPs in the thymidine groups (Table S9).

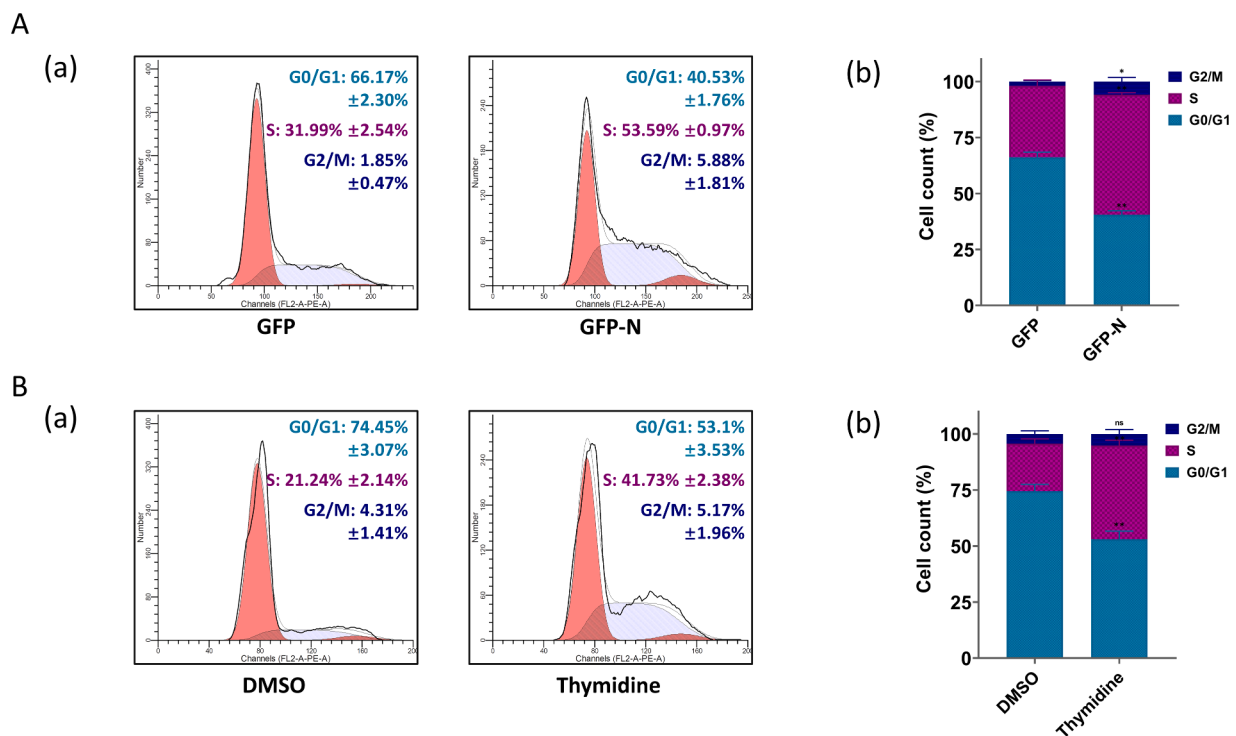


Fig. 2. The flow cytometry analysis of the PEDV N/thymidine-induced S-phase arrested Vero E6 cells. A. Flow cytometry analysis of the PEDV N-induced S-phase arrested Vero E6 cells. The Vero E6 cells were transfected with GFP-N or GFP plasmids for 24 h. The cell cycle distribution was analyzed by flow cytometry (a). The percentage of cells in S-phase was analyzed and presented in the graph (b). B. The flow cytometry analysis of the thymidine-induced S-phase arrested Vero E6 cells. The Vero E6 cells were arrested in the S-phase following treatment with thymidine or DMSO. The cell cycle distribution was analyzed by flow cytometry (a). The percentage of cells in S-phase was analyzed and is shown in the graph (b). The results are representative of three independent experiments (means \pm SD). * $P < 0.05$; ** $P < 0.01$. The P values were calculated using a Student's t test.

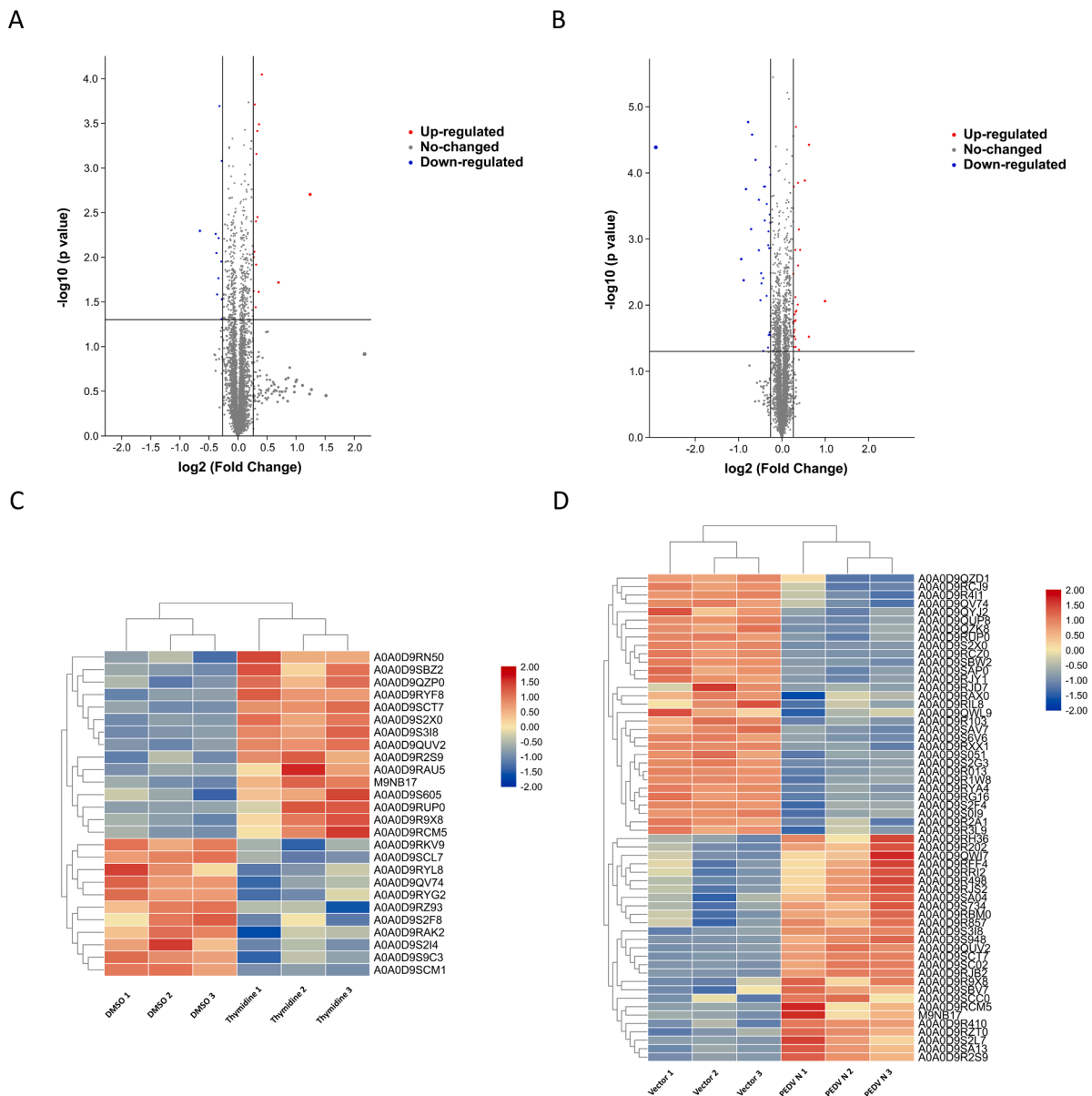


Fig. 3. Changes in the level of differentially expressed protein (DEP) expression. (A) Volcano plot of the differentially expressed genes between the cell lines treated with or without thymidine. (B) Volcano plot of the differentially expressed genes between GFP-N and GFP expressed cell lines. (C) A heatmap of 26 genes showing significant differential expression between cell lines treated with or without thymidine. (D) Heatmap of 58 genes exhibiting significant differential expression between GFP-N and GFP expressed cells lines. Each row represents a gene. Red indicates increased expression. Blue indicates decreased expression.

There were 45 proteins that were unique DEPs in the PEDV N group (Table S10). The GO and KEGG pathway annotations of the shared DEPs and unique DEPs are shown in Fig. 5 (Table S11–S13). The DEPs identified in the PEDV N group were primarily focused on cell growth and metabolic regulation-associated proteins, DNA replication, transcription, and protein synthesis of host cells. The PPI network analysis of the 45 unique DEPs in the PEDV N group revealed that three groups of proteins, RPL18-RPL10-RPL15-WDR20-PACS2, COPZ1-ARF4-TBC1D30-ACTRT1-IGBP1, and DCP1B-PCBP2-GTF2E1-SMARCD1, were found to interact strongly with each other proteins (Fig. 6A). Many viruses can modulate the host cell translation system to synthesize their own viral proteins by targeting the ribosomal proteins. To better understand how the 60S ribosomal protein L18 (RPL18) interacts with the cellular proteins and affects cell functions, the PPI network related to “replication and transcription” was established by searching the String database. The results indicated that RPL18 exhibited a strong interaction

with 69 replication/transcription-associated proteins that include 38 60S ribosomal proteins, 28 40S ribosomal proteins, eukaryotic initiation factor 6 (eIF6), ubiquitin-52 amino acid fusion protein (Uba52), and eukaryotic elongation factor 2 (eEF2), which form intricate protein-protein interaction networks (Fig. 6B).

3.3. Validation of the level of RPL18 protein expression in PEDV N-induced S-phase arrested cells and PEDV-infected IPEC-J2 cells

To investigate the level of the RPL-18 protein expression in PEDV N-induced S-phase arrested cells and PEDV-infected cells, the PEDV N protein-induced S-phase arrested Vero E6, the PEDV N protein-induced S-phase arrested IPEC-J2 cells and PEDV strain CV777-infected IPEC-J2 cells were prepared, respectively. The level of RPL18 protein expression in the prepared cells was subjected to detection and analysis via Western blot. The results indicated that the level of the RPL18 protein expression

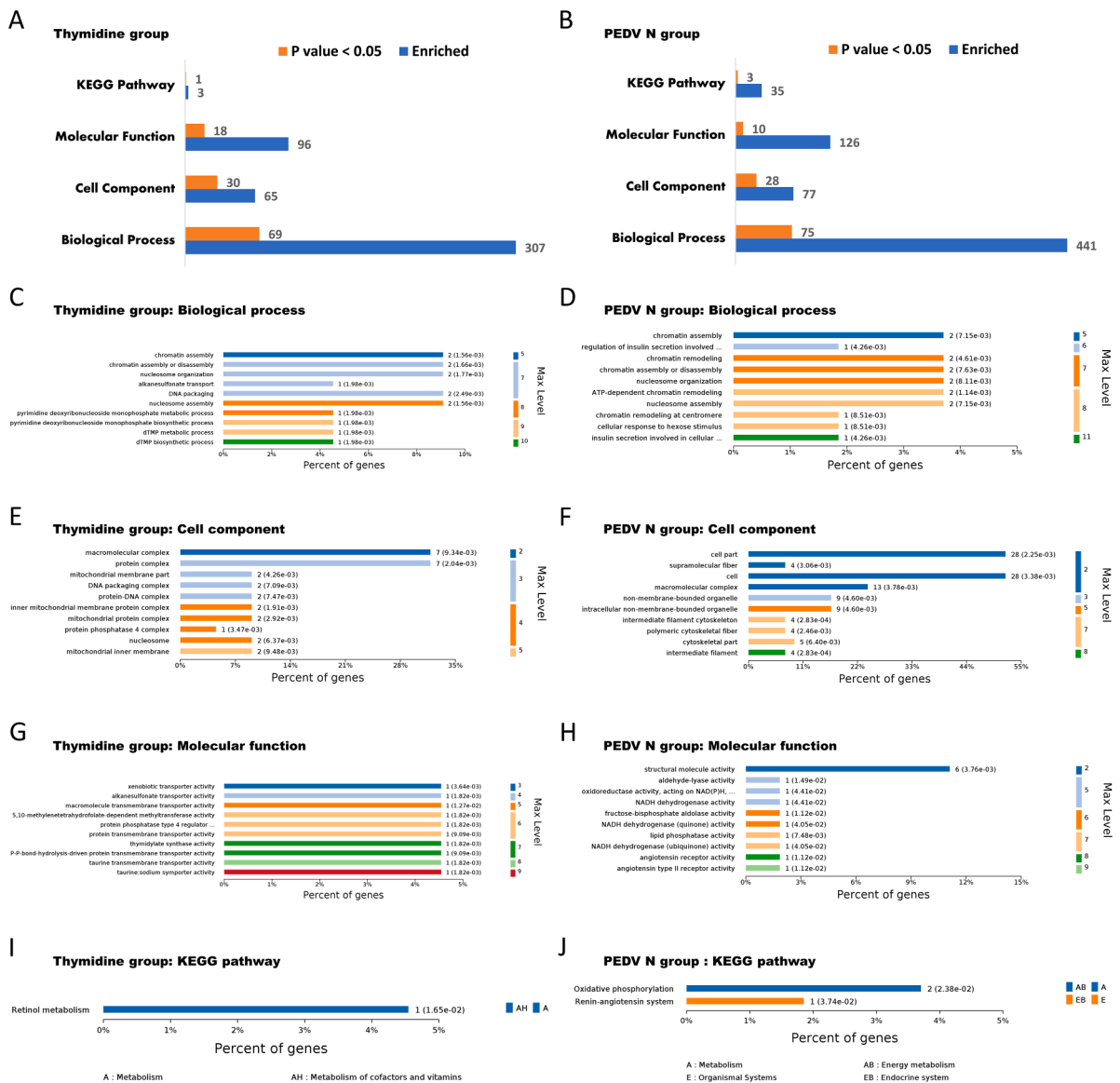


Fig. 4. Functional characterization of significantly differently expressed proteins of the thymidine groups and PEDV N groups. A and B. Functional classification of significantly differently expressed proteins. C and D. Biological process. E and F. Cellular components. G and H. Molecular function. I and J. KEGG pathway.

in the PEDV N protein-induced S-phase arrested Vero E6 cells and the PEDV N protein-induced S-phase arrest IPEC-J2 cells were all significantly higher than that of the GFP control group ($P < 0.01$). In the Vero E6 cells, the ratio of the level of RPL18 protein expression reached 1.91 between PEDV GFP-N group and GFP control group (Fig. 7A). In the IPEC-J2 cells, the level of RPL18 protein expression the PEDV GFP-N group was 1.81-fold that of the GFP control group (Fig. 7B). The level of RPL18 protein expression in the IPEC-J2 cells infected with PEDV strain CV777 were significantly higher than that in the DMEM control group ($P < 0.01$). The ratio of the level of RPL18 protein expression reached 1.67 between the PEDV group and DMEM control group (Fig. 7C). These results demonstrate that the expression levels of the RPL18 protein exhibited a significant increase in PEDV N-induced S-phase arrested cells and PEDV-infected cells, which is in line with the results of the TMT-labeled quantitative proteomic analysis.

3.4. Effects of the RPL18 protein on PEDV replication

To investigate influence of RPL18 protein overexpression on PEDV replication, the swine RPL18 gene was successfully expressed on porcine

IPEC-J2 intestinal epithelial cells using the eukaryotic expression vector, pAcGFP1-C1 (Fig. 8A). Furthermore, the viral titers of the PEDV classic strain CV777 and variant strain HM2017 were evaluated in RPL18-overexpressed IPEC-J2 cells, respectively. The results indicated that the viral titer of the PEDV classic strain CV777 in RPL18-overexpressed IPEC-J2 cells reached $4.63 \pm 0.13 \log_{10}$ TCID₅₀/mL, which was higher than that of the GFP control group ($4.17 \pm 0.19 \log_{10}$ TCID₅₀/mL) ($P < 0.05$, Fig. 8B). The viral titer of the PEDV variant HM2017 strain in the RPL18-overexpressed IPEC-J2 cells reached $5.42 \pm 0.07 \log_{10}$ TCID₅₀/mL, which was higher than that of the GFP control group ($4.54 \pm 0.07 \log_{10}$ TCID₅₀/mL) ($P < 0.01$, Fig. 8C). These results revealed that RPL18 protein overexpression could significantly enhance PEDV replication.

To investigate the effect of RPL18 protein down-regulation on PEDV replication, three siRNA duplexes targeting the RPL18 gene, termed sus-17, sus-238, and sus-482, were synthesized, respectively. The small interfering RNA sus-482 that significantly down-regulated expression of the RPL18 protein in the PEDV-uninfected IPEC-J2 cells was identified by western blot (Fig. 8D). Moreover, the viral titers of PEDV classic strain CV777 and variant strain HM2017 were evaluated in the RPL18-silenced IPEC-J2 cells, respectively. The results indicated that the viral

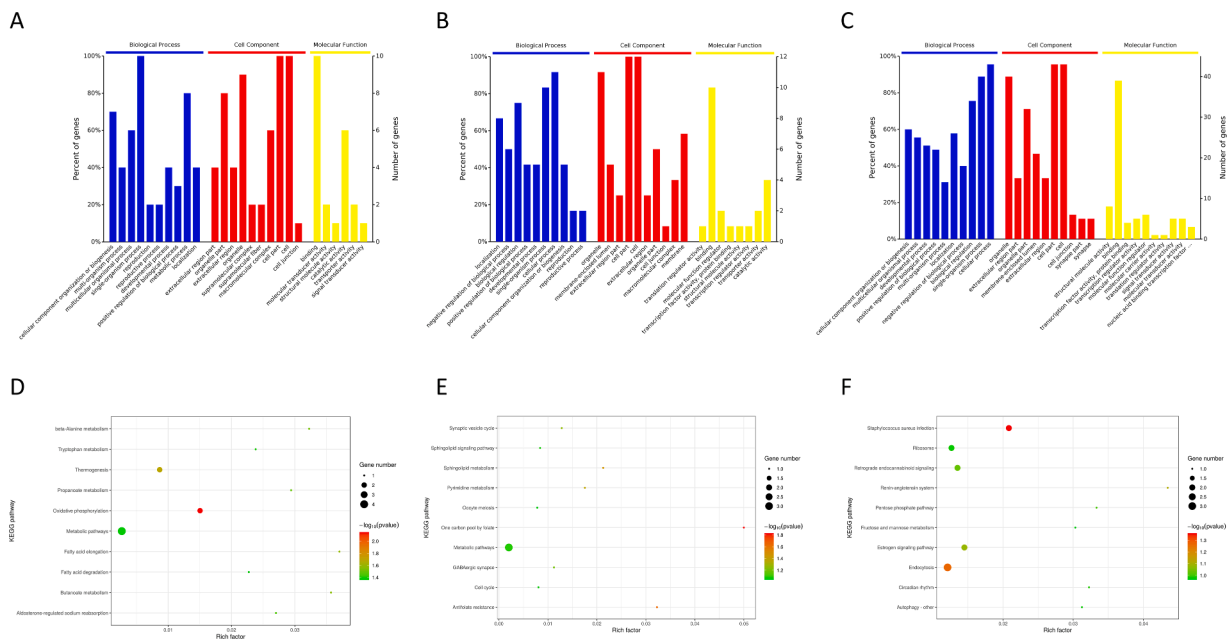


Fig. 5. GO and KEGG pathway annotations of the DEPs. A and D. The shared DEPs between the thymidine and PEDV N groups. B and E. The unique DEPs in the thymidine group. C and F. The unique DEPs in the PEDV N group.

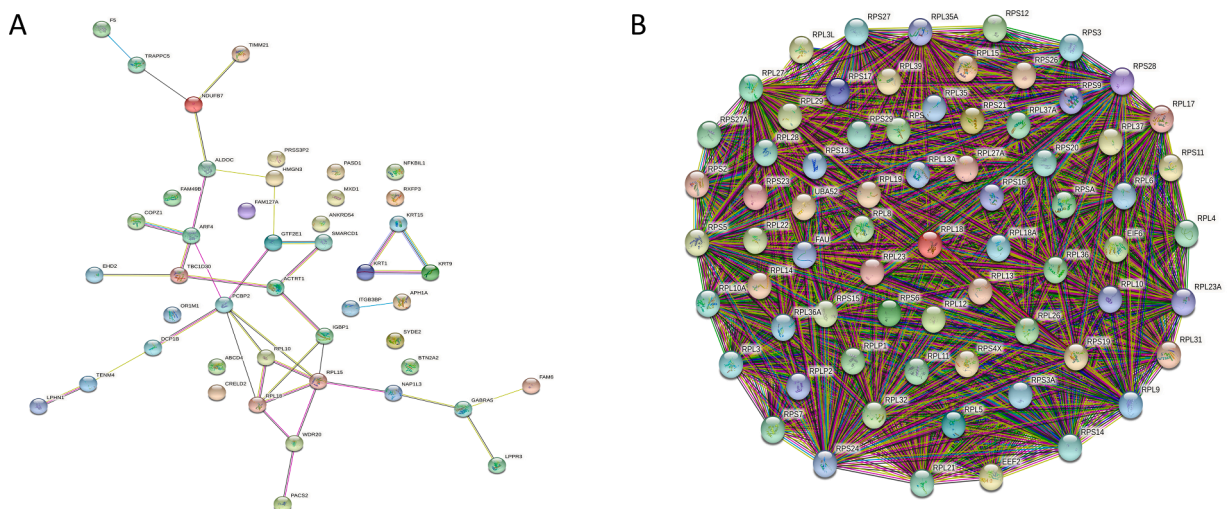


Fig. 6. Protein-protein interaction (PPI) network analysis of the unique DEPs in the PEDV N group. A. The PPI network analysis of the 45 unique DEPs in the PEDV N group. B. PPI network analysis of the RPL18 interaction with replication/transcription-associated proteins.

titers of the PEDV classic strain CV777 in the RPL18-silenced IPEC-J2 cells reached $5.13 \pm 0.13 \log_{10}$ TCID₅₀/mL, which were lower than that of the GFP control group ($5.58 \pm 0.19 \log_{10}$ TCID₅₀/mL) ($P < 0.05$, Fig. 8E). The viral titers of the PEDV variant strain HM2017 in the RPL18-silenced IPEC-J2 cells reached $6.21 \pm 0.19 \log_{10}$ TCID₅₀/mL, which were lower than that of the GFP control group ($6.96 \pm 0.26 \log_{10}$ TCID₅₀/mL) ($P < 0.01$, Fig. 8F). These results revealed that down-regulated RPL18 protein expression could significantly inhibit PEDV replication. These data demonstrate that up-regulated RPL18 protein expression could enhance PEDV replication when the PEDV N protein interacts with p53 to induce host cell cycle arrest during the S-phase.

4. Discussion

Deregulation of the cell cycle is a common strategy adopted by many RNA (and DNA) viruses, which aims to exploit the host cell machinery to create a more favorable environment for survival (Bagga and Bouchard,

2014; Bogdanow et al., 2021; Liu et al., 2020). Coronavirus (CoV) has evolved multiple mechanisms that induce cell cycle arrest to ensure sufficient resources and cellular conditions favorable for viral replication to enhance replication efficiency (Chen et al., 2004; Su et al., 2020a; Surjit et al., 2006). However, the mechanism by which viral replication is increased in the CoV-induced host cell cycle arrest cells remain unknown. The CoV N protein is a multifunctional protein that forms complexes with genomic RNA, interacts with the viral membrane protein during virion assembly, and plays a critical role in enhancing the efficiency of virus transcription and assembly (McBride et al., 2014). Moreover, the CoV N protein exhibits cell cycle-dependent nucleolar localization, involving modulation of the host cell cycle (Cawood et al., 2007; Chen et al., 2002). In previous studies, we identified a key mechanism underlying PEDV N-induced S-phase arrest to be that the interaction between PEDV N protein and p53 modulates cell cycle arrest at S-phase to promote viral replication by activating p53-DREAM pathway. Furthermore, this S-phase arrest was found to be dependent

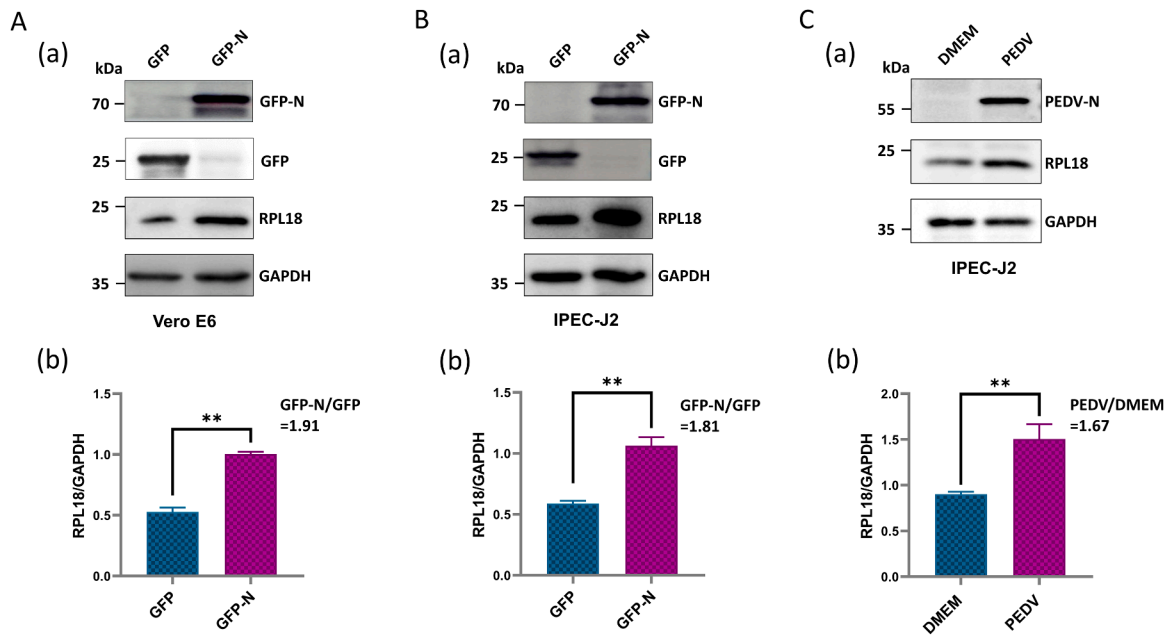


Fig. 7. Validation of the level of RPL18 protein expression in PEDV N-induced S-phase arrested cells and PEDV-infected IPEC-J2 cells. A and B. The level of RPL18 expression in Vero E6 (A) and IPEC-J2 (B) cells expressing GFP-N. The level of RPL18 expression in cells expressing GFP-N or GFP was determined by Western blot using anti-RPL18 antibodies (a). The level of RPL18 expression was analyzed and is presented in the graph (b). C. The level of RPL18 expression in PEDV-infected IPEC-J2 cells. The level of RPL18 expression in IPEC-J2 cells infected with or without PEDV was determined by Western blot using anti-RPL18 antibodies (a). The level of RPL18 expression was analyzed and is presenting in the graph (b). The results are representative of three independent experiments (means \pm SD). * $P < 0.05$; ** $P < 0.01$. The P values were calculated using a Student's t test.

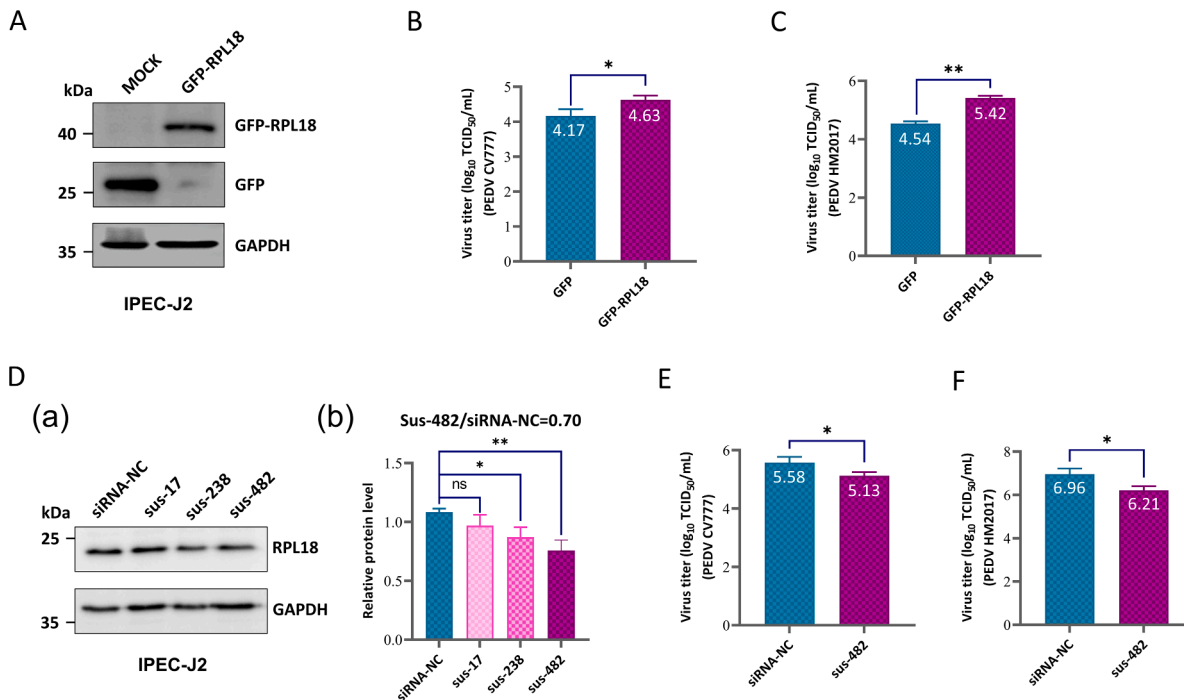


Fig. 8. Effects of the RPL18 protein on PEDV replication. A. Verification of RPL18 overexpression in IPEC-J2 cells. The level of RPL18 expression in IPEC-J2 cells expressing GFP-RPL18 and GFP were determined by Western blot using anti-RPL18 antibodies. B and C. Effects of RPL18 overexpression on PEDV CV777 (B) and HM2017 (C) strain replication. Vero E6 cells were transfected with GFP-RPL18 or GFP plasmids. After 24 hpt, the cells were infected with PEDV for 48 h. The cells and supernatants were collected for the TCID₅₀ test. D. Verification of siRNA inhibition of RPL18 in IPEC-J2 cells. The level of RPL18 expression in IPEC-J2 cells treated with siRNA-RPL18 and siRNA-NC was determined by Western blot with anti-RPL18 antibodies (a). The level of RPL18 expression was analyzed and is shown in the graph (b). E. Effects of RPL18 knockdown on PEDV CV777 strain replication. Vero E6 cells were transfected with GFP-RPL18 or GFP plasmids. After 24 hpt, the cells were infected with PEDV CV777 strain for 48 h. The cells and supernatants were collected for the TCID₅₀ test. F. Effects of RPL18 knockdown on PEDV HM2017 strain replication. The results are representative of three independent experiments (means \pm SD). * $P < 0.05$; ** $P < 0.01$. The P values were calculated using a Student's t test.

on the nuclear localization signal N^{S71-T90} and the N-p53 binding domain N^{S171-N194} of the PEDV N protein (Su et al., 2021). In the current study, TMT-labeled quantitative proteomic technology was employed to characterize the protein expression profile of PEDV N protein-induced S-phase arrested Vero E6 cells and thymidine-induced S-phase arrested Vero E6 cells. A comparison between the PEDV N group and thymidine group revealed unique DEPs of the PEDV N protein-induced S-phase arrested Vero E6 cells. We comprehensively elucidated the cellular components, biological processes, molecular functions, signaling pathways, and PPIs of the DEPs identified in the PEDV N group. The 60S ribosomal protein, L18 (RPL18), is primarily involved in ribosomal biosynthesis and cellular growth and proliferation, and exhibited significantly up-regulated expression in the PEDV N protein-induced S-phase arrested Vero E6/IPEC-J2 cells and PEDV-infected IPEC-J2 cells ($P < 0.05$). Further studies revealed that up-regulated RPL18 expression significantly enhanced the viral replication of PEDV classical and variant strains. Our study revealed an important mechanism regarding the formation of a favorable environment for enhancing viral replication attributed to the interaction between the coronavirus PEDV N protein and p53 to induce host cell cycle arrest during S-phase. These data provide new insight into the mechanism by which coronavirus N protein induces host cell cycle arrest to enhance viral replication. Our findings may aid in novel antiviral strategy design for coronaviruses.

Viruses induce profound changes in the host cells they infect. Understanding these perturbations will assist in designing better therapeutics to combat viral infection. System-based proteomic assays now provide an unprecedented opportunity to monitor a large number of cellular proteins (Allgoewer et al., 2021; Coombs, 2020; Meignie et al., 2021; Zecha et al., 2020). TMT-based quantitative proteomic technology involves tagging differentially treated samples with various markers that may be differentiated by mass (Thompson et al., 2003). In addition, TMT coupled with LC-MS/MS allows for a simultaneous and quantitative comparison of thousands of proteins in complex mixtures, thereby representing a powerful approach to uncovering virus-induced protein alterations and virus-host protein interactions during the progression of viral infection (Coombs, 2020; Praissman and Wells, 2021). Shen et al. (2020) used the newest generation 16-plex TMTpro reagents to reveal characteristic protein and metabolite changes in the sera of severe COVID-19 patients, which might be used in the selection of potential blood biomarkers to evaluate severity (Shen et al., 2020). At present, it has been shown that coronaviruses have evolved multiple mechanisms to induce cell cycle arrest to create a cellular microenvironment that favors viral replication (Su et al., 2021). However, there are no reports of the panoramic changes in host cells when coronavirus-mediated host cells are in a state of cell cycle arrest. In this study, we used TMT-based quantitative proteomics technology for the first time to comprehensively reveal the changes in protein expression in cells in a state of cell cycle S-phase arrest mediated by the PEDV N protein. The resulting data provides a powerful reference for the molecular mechanism by which virus-mediated cell cycle arrest enhances virus replication, especially in coronaviruses. However, one inevitable challenge is that a large number of the experimentally-associated target proteins are obtained due to the high-throughput characteristics of quantitative proteomics technology and the complexity of virus-host interactions. The most interesting protein candidates are associated with the substantial limitation of further validating whether each target protein is involved in the interaction between virus and host cells. Thymidine is a DNA synthesis inhibitor that can arrest cell at the G1/S boundary, prior to DNA replication (Chen and Deng, 2018). Thymidine has been widely used to study the mechanisms involved in the regulation of cell cycle progression through cell synchronization (Su et al., 2021; Surani et al., 2021). In our study, a total of 15 DEPs common between the thymidine group and PEDV N group were eliminated from the 58 DEPs identified in the PEDV N group using thymidine as the cell cycle arrest control group. This process generated unique DEPs of the PEDV N-induced S-phase arrested cells. The ribosomal protein, L18, was efficiently selected as a

highlighted target responsible for the formation of a favorable environment, which enhances viral replication when the coronavirus PEDV N protein interacts with p53 to induce host cell cycle arrest at S-phase.

Ribosomal proteins (RPs) are the principal components of cell ribosomes, which are involved in 80 various types of ribosomal proteins. In addition, RPs play an important regulatory role in ribosomal biosynthesis, as well as cellular growth and proliferation. Accumulating studies have revealed that in the co-evolution process between virus and host interactions, several viruses were able to modulate the endogenous translation pathway of the host cell to synthesize their own viral proteins for replication and proliferation by "hijacking" host RPs (Cervantes-Salazar et al., 2015; Jefferson et al., 2014). Of the 5709 proteins identified in our study, a total of 124 RPs were found in the PEDV N-induced S-phase arrested cells and the thymidine-induced S-phase arrested cells. These data strongly support RPs as the main participants in the biological regulation of host cells upon S-phase arrest. Further analysis indicated that the 60S ribosomal proteins L10 (RPL10), L15 (RPL15), and L18 (RPL18) were unique DEPs in the PEDV N-induced Vero E6 cell S-phase arrested cells compared with the thymidine control group. In addition, the RPL18 exhibited a strong interaction with 69 replication/transcription-associated proteins, including 38 60S ribosomal proteins, 28 40S ribosomal proteins, eukaryotic initiation factor 6 (eIF6), ubiquitin-52 amino acid fusion protein (Uba52), and eukaryotic elongation factor 2 (eEF2). RPL18 aroused our interest to further explore the molecular mechanism by which viral replication was promoted in the PEDV N-mediated S-phase arrested host cells. The double-stranded RNA (dsRNA)-activated protein kinase (PKR) is essential for the regulation of cellular growth. Studies have indicated that RPL18 has been shown to interact with PKR, inhibiting PKR phosphorylation and the alpha subunit of eukaryotic translation initiation factor 2 (eIF-2 α). The level of PKR and eIF-2 α phosphorylation positively regulates the formation of stress granules (SGs) via TIA-1 and G3BP1/2. SGs represent an aggregation product of the translation initiation complex in the cytoplasm and plays an important role in gene expression and homeostasis. In general, viral infection could induce the host cells to promote the formation of SGs. The host cells halt their own translation when SG production increases in the cells, which inhibits viral replication; however, SARS-CoV-2, MERS-CoV, and other viruses can inhibit SG formation and create cellular conditions favorable for viral replication (Nakagawa et al., 2018; Zheng et al., 2021). In the current study, RPL18 was confirmed to be up-regulated in the PEDV N-induced S-phase arrested cells. Moreover, the up-regulated RPL18 expression significantly promoted PEDV replication. Our findings are in line with the previous conclusions. Moreover, accumulating studies have suggested that the "RPL18-PKR/eIF2 α -SG-virus replication" pathway may represent a potential common mechanism regarding increased viral replication in the virus-induced S-phase arrested host cells (Burke et al., 2019; Busnadiago et al., 2012; Wang et al., 2018).

In conclusion, TMT-labeled quantitative proteomics was used to systematically identify the DEP profiles of the PEDV N-induced S-phase arrested cells, revealing a mechanism by which virus replication is enhanced during S-phase arrest of host cells mediated by the PEDV N protein. The level of the 60S ribosomal protein, RPL18, expression was up-regulated in the PEDV N protein-induced S-phase arrested host cells, which promoted viral replication. Our study provides novel insight into the increased viral replication observed in PEDV N protein-induced S-phase arrested cells and the design of novel antiviral strategies of PEDV. Our results further expand the understanding of how coronaviruses regulate the host cell cycle to create a favorable environment for virus replication.

CRedit authorship contribution statement

Qinghe Zhu: Methodology, Writing – original draft. **Mingjun Su:** Methodology, Writing – original draft. **Shan Wei:** Methodology. **Da Shi:** Formal analysis. **Lu Li:** Formal analysis. **Jun Wang:** Formal analysis.

Haibo Sun: Formal analysis. **Meijiao Wang:** Formal analysis. **Chunqiu Li:** Formal analysis. **Donghua Guo:** Conceptualization, Visualization. **Dongbo Sun:** Conceptualization, Visualization, Writing – original draft.

Declaration of Competing Interest

The authors declare that they have no conflicts of interest.

Data availability

No data was used for the research described in the article.

Acknowledgments

The study was supported by the National Natural Science Foundation of China (grant no.31873011/3210190544), the National Funds for Supporting Reform and Development of Heilongjiang Provincial Colleges and Universities (grant no. 2022010009), and the Key Research and Development Program of Heilongjiang Province (grant no. GA21B004).

Supplementary materials

Supplementary material associated with this article can be found, in the online version, at doi:[10.1016/j.virusres.2022.198916](https://doi.org/10.1016/j.virusres.2022.198916).

References

- Allgoewer, K., Maity, S., Zhao, A., Lashua, L., Ramgopal, M., Balkaran, B.N., Liu, L., Purushwani, S., Arevalo, M.T., Ross, T.M., Choi, H., Ghedin, E., Vogel, C., 2021. New proteomic signatures to distinguish between zika and dengue infections. *Mol. Cell. Proteom.* 20, 100052 <https://doi.org/10.1016/j.mcp.2021.100052>.
- Bagga, S., Bouchard, M.J., 2014. Cell cycle regulation during viral infection. *Methods Mol. Biol.* 1170, 165–227. https://doi.org/10.1007/978-1-4939-0888-2_10.
- Bogdanow, B., Phan, Q.V., Wiebusch, L., 2021. Emerging mechanisms of G1/S cell cycle control by human and mouse cytomegaloviruses. *mBio* 12 (6), e0293421. <https://doi.org/10.1128/mBio.02934-21>.
- Bouhaddou, M., Memon, D., Meyer, B., White, K.M., Rezelj, V.V., Correa Marrero, M., Polacco, B.J., Melnyk, J.E., Ulferts, S., Kaake, R.M., Batra, J., Richards, A.L., Stevenson, E., Gordon, D.E., Rojic, A., Obernier, K., Fabius, J.M., Soucheray, M., Miorin, L., Moreno, E., Koh, C., Tran, Q.D., Hardy, A., Robinot, R., Vallet, T., Nilsson-Payant, B.E., Hernandez-Armenta, C., Dunham, A., Weigang, S., Knerr, J., Modak, M., Quintero, D., Zhou, Y., Dugourd, A., Valdeolivas, A., Patil, T., Li, Q., Huttenhain, R., Cakir, M., Muralidharan, M., Kim, M., Jang, G., Tutuncuoglu, B., Hiatt, J., Guo, J.Z., Xu, J., Bouhaddou, S., Mathy, C.J.P., Gaulton, A., Mannes, E.J., Felix, E., Shi, Y., Goff, M., Lim, J.K., McBride, T., O'Neal, M.C., Cai, Y., Chang, J.C.J., Broadhurst, D.J., Klippsten, S., De Wit, E., Leach, A.R., Kortemme, T., Shoichet, B., Ott, M., Saez-Rodriguez, J., tenOever, B.R., Mullins, R.D., Fischer, E.R., Kochs, G., Grosse, R., Garcia-Sastre, A., Vignuzzi, M., Johnson, J.R., Shokat, K.M., Swaney, D. L., Beltrao, P., Krogan, N.J., 2020. The global phosphorylation landscape of SARS-CoV-2 infection. *Cell* 182 (3), 685–712. <https://doi.org/10.1016/j.cell.2020.06.034> e619.
- Burke, J.M., Moon, S.L., Matheny, T., Parker, R., 2019. RNase L reprograms translation by widespread mRNA turnover escaped by antiviral mRNAs. *Mol. Cell* 75 (6), 1203–1217. <https://doi.org/10.1016/j.molcel.2019.07.029> e1205.
- Busnadiego, I., Maestre, A.M., Rodriguez, D., Rodriguez, J.F., 2012. The infectious bursal disease virus RNA-binding VP3 polypeptide inhibits PKR-mediated apoptosis. *PLoS One* 7 (10), e46768. <https://doi.org/10.1371/journal.pone.0046768>.
- Cawood, R., Harrison, S.M., Dove, B.K., Reed, M.L., Hiscox, J.A., 2007. Cell cycle dependent nucleolar localization of the coronavirus nucleocapsid protein. *Cell Cycle* 6 (7), 863–867. <https://doi.org/10.4161/cc.6.7.4032>.
- Cervantes-Salazar, M., Angel-Ambrocio, A.H., Soto-Acosta, R., Bautista-Carbajal, P., Hurtado-Monzon, A.M., Alcaraz-Estrada, S.L., Ludert, J.E., Del Angel, R.M., 2015. Dengue virus NS1 protein interacts with the ribosomal protein RPL18: this interaction is required for viral translation and replication in Huh-7 cells. *Virology* 484, 113–126. <https://doi.org/10.1016/j.virol.2015.05.017>.
- Chen, C.J., Sugiyama, K., Kubo, H., Huang, C., Makino, S., 2004. Murine coronavirus nonstructural protein p28 arrests cell cycle in G0/G1 phase. *J. Virol.* 78 (19), 10410–10419. <https://doi.org/10.1128/JVI.78.19.10410-10419.2004>.
- Chen, G., Deng, X., 2018. Cell synchronization by double thymidine block. *Bio Protocol* 8 (17). <https://doi.org/10.21769/BioProtoc.2994>.
- Chen, H., Wurm, T., Britton, P., Brooks, G., Hiscox, J.A., 2002. Interaction of the coronavirus nucleoprotein with nucleolar antigens and the host cell. *J. Virol.* 76 (10), 5233–5250. <https://doi.org/10.1128/jvi.76.10.5233-5250.2002>.
- Coombs, K.M., 2020. Update on proteomic approaches to uncovering virus-induced protein alterations and virus-host protein interactions during the progression of viral infection. *Expert Rev. Proteom.* 17 (7–8), 513–532. <https://doi.org/10.1080/14789450.2020.1821656>.
- Cui, J., Li, F., Shi, Z.L., 2019. Origin and evolution of pathogenic coronaviruses. *Nat. Rev. Microbiol.* 17 (3), 181–192. <https://doi.org/10.1038/s41579-018-0118-9>.
- Ding, L., Huang, Y., Dai, M., Zhao, X., Du, Q., Dong, F., Wang, L., Huo, R., Zhang, W., Xu, X., Tong, D., 2013. Transmissible gastroenteritis virus infection induces cell cycle arrest at S and G2/M phases via p53-dependent pathway. *Virus Res.* 178 (2), 241–251. <https://doi.org/10.1016/j.virusres.2013.09.036>.
- Ding, L., Huang, Y., Du, Q., Dong, F., Zhao, X., Zhang, W., Xu, X., Tong, D., 2014. TGEV nucleocapsid protein induces cell cycle arrest and apoptosis through activation of p53 signaling. *Biochem. Biophys. Res. Commun.* 445 (2), 497–503. <https://doi.org/10.1016/j.bbrc.2014.02.039>.
- Gerds, V., Zakhartchouk, A., 2017. Vaccines for porcine epidemic diarrhea virus and other swine coronaviruses. *Vet. Microbiol.* 206, 45–51. <https://doi.org/10.1016/j.vetmic.2016.11.029>.
- Jefferson, M., Donaszi-Ivanov, A., Pollen, S., Dalmay, T., Saalbach, G., Powell, P.P., 2014. Host factors that interact with the pestivirus N-terminal protease, Npro, are components of the ribonucleoprotein complex. *J. Virol.* 88 (18), 10340–10353. <https://doi.org/10.1128/JVI.00984-14>.
- Li, Y., Si, H.R., Zhu, Y., Xie, N., Li, B., Zhang, X.P., Han, J.F., Bao, H.H., Yang, Y., Zhao, K., Hou, Z.Y., Cheng, S.J., Zhang, S.H., Shi, Z.L., Zhou, P., 2022. Characteristics of SARS-CoV-2 transmission in a medium-sized city with traditional communities during the early COVID-19 epidemic in China. *Virol. Sin.* 37 (2), 187–197. <https://doi.org/10.1016/j.virs.2022.01.030>.
- Li, C., Su, M., Yin, B., Guo, D., Wei, S., Kong, F., Feng, L., Wu, R., Sun, D., 2019. Integrin alphavbeta3 enhances replication of porcine epidemic diarrhea virus on Vero E6 and porcine intestinal epithelial cells. *Vet. Microbiol.* 237, 108400. <https://doi.org/10.1016/j.vetmic.2019.108400>.
- Liu, S., Liu, H., Kang, J., Xu, L., Zhang, K., Li, X., Hou, W., Wang, Z., Wang, T., 2020. The severe fever with thrombocytopenia syndrome virus NSs protein interacts with CDK1 to sever G2 cell cycle arrest and positively regulate viral replication. *J. Virol.* 94 (6) <https://doi.org/10.1128/JVI.01575-19>.
- McBride, R., van Zyl, M., Fielding, B.C., 2014. The coronavirus nucleocapsid is a multifunctional protein. *Viruses* 6 (8), 2991–3018. <https://doi.org/10.3390/v6082991>.
- Meignie, A., Combredet, C., Santolini, M., Kovacs, I.A., Douche, T., Gianetto, Q.G., Eun, H., Matondo, M., Jacob, Y., Grailhe, R., Tangy, F., Komarova, A.V., 2021. Proteomic analysis uncovers measles virus protein C interaction with p65-iASPP protein complex. *Mol. Cell. Proteom.* 20, 100049. <https://doi.org/10.1016/j.mcp.2021.100049>.
- Nakagawa, K., Narayanan, K., Wada, M., Makino, S., 2018. Inhibition of stress granule formation by middle east respiratory syndrome coronavirus 4a accessory protein facilitates viral translation, leading to efficient virus replication. *J. Virol.* 92 (20) <https://doi.org/10.1128/JVI.00902-18>.
- Nascimento, R., Costa, H., Parkhouse, R.M., 2012. Virus manipulation of cell cycle. *Protoplasma* 249 (3), 519–528. <https://doi.org/10.1007/s00709-011-0327-9>.
- Nemeth, B., Fasseeh, A., Molnar, A., Bitter, I., Horvath, M., Koczian, K., Gotze, A., Nagy, B., 2018. A systematic review of health economic models and utility estimation methods in schizophrenia. *Expert Rev. Pharmacoecon. Outcomes Res.* 18 (3), 267–275. <https://doi.org/10.1080/14737167.2018.1430571>.
- Praissman, J.L., Wells, L., 2021. Proteomics-based insights into the SARS-CoV-2-Mediated COVID-19 pandemic: a review of the first year of research. *Mol. Cell. Proteom.* 20, 100103. <https://doi.org/10.1016/j.mcp.2021.100103>.
- Shen, B., Yi, X., Sun, Y., Bi, X., Du, J., Zhang, C., Quan, S., Zhang, F., Sun, R., Qian, L., Ge, W., Liu, W., Liang, S., Chen, H., Zhang, Y., Li, J., Xu, J., He, Z., Chen, B., Wang, J., Yan, H., Zheng, Y., Wang, D., Zhu, J., Kong, Z., Kang, Z., Liang, X., Ding, X., Ruan, G., Xiang, N., Cai, X., Gao, H., Li, L., Li, S., Xiao, Q., Lu, T., Zhu, Y., Liu, H., Chen, H., Guo, T., 2020. Proteomic and metabolomic characterization of COVID-19 patient sera. *Cell* 182 (1), 59–72. <https://doi.org/10.1016/j.cell.2020.05.032> e15.
- Shi, Z., 2021. [From SARS, MERS to COVID-19: a journey to understand bat coronaviruses]. *Bull. Acad. Natl. Med.* 205 (7), 732–736. <https://doi.org/10.1016/j.banm.2021.05.008>.
- Su, M., Chen, Y., Qi, S., Shi, D., Feng, L., Sun, D., 2020a. A mini-review on cell cycle regulation of coronavirus infection. *Front. Vet. Sci.* 7, 586826. <https://doi.org/10.3389/fvets.2020.586826>.
- Su, M., Li, C., Qi, S., Yang, D., Jiang, N., Yin, B., Guo, D., Kong, F., Yuan, D., Feng, L., Sun, D., 2020b. A molecular epidemiological investigation of PEDV in China: characterization of co-infection and genetic diversity of S1-based genes. *Transbound. Emerg. Dis.* 67 (3), 1129–1140. <https://doi.org/10.1111/tbed.13439>.
- Su, M., Shi, D., Xing, X., Qi, S., Yang, D., Zhang, J., Han, Y., Zhu, Q., Sun, H., Wang, X., Wu, H., Wang, M., Wei, S., Li, C., Guo, D., Feng, L., Sun, D., 2021. Coronavirus porcine epidemic diarrhea virus nucleocapsid protein interacts with p53 to induce cell cycle arrest in S-Phase and promotes viral replication. *J. Virol.* 95 (16), e0018721. <https://doi.org/10.1128/JVI.00187-21>.
- Sun, D., Wang, X., Wei, S., Chen, J., Feng, L., 2016. Epidemiology and vaccine of porcine epidemic diarrhea virus in China: a mini-review. *J. Vet. Med. Sci.* 78 (3), 355–363. <https://doi.org/10.1292/jvms.15-0446>.
- Surani, A.A., Colombo, S.L., Barlow, G., Foulds, G.A., Montiel-Duarte, C., 2021. Optimizing cell synchronization using nocodazole or double thymidine block. *Methods Mol. Biol.* 2329, 111–121. https://doi.org/10.1007/978-1-0716-1538-6_9.
- Surjit, M., Liu, B., Chow, V.T., Lal, S.K., 2006. The nucleocapsid protein of severe acute respiratory syndrome-coronavirus inhibits the activity of cyclin-cyclin-dependent kinase complex and blocks S phase progression in mammalian cells. *J. Biol. Chem.* 281 (16), 10669–10681. <https://doi.org/10.1074/jbc.M509233200>.

- Thompson, A., Schafer, J., Kuhn, K., Kienle, S., Schwarz, J., Schmidt, G., Neumann, T., Johnstone, R., Mohammed, A.K., Hamon, C., 2003. Tandem mass tags: a novel quantification strategy for comparative analysis of complex protein mixtures by MS/MS. *Anal. Chem.* 75 (8), 1895–1904. <https://doi.org/10.1021/ac0262560>.
- Wang, B., Duan, X., Fu, M., Liu, Y., Wang, Y., Li, X., Cao, H., Zheng, S.J., 2018. The association of ribosomal protein L18 (RPL18) with infectious bursal disease virus viral protein VP3 enhances viral replication. *Virus Res.* 245, 69–79. <https://doi.org/10.1016/j.virusres.2017.12.009>.
- Wang, Q., Vlasova, A.N., Kenney, S.P., Saif, L.J., 2019. Emerging and re-emerging coronaviruses in pigs. *Curr. Opin. Virol.* 34, 39–49. <https://doi.org/10.1016/j.coviro.2018.12.001>.
- Wang, Y., Liu, M., Shen, Y., Ma, Y., Li, X., Zhang, Y., Liu, M., Yang, X.L., Chen, J., Yan, R., Luan, D., Wang, Y., Chen, Y., Wang, Q., Lin, H., Li, Y., Wu, K., Zhu, T., Zhao, J., Lu, H., Wen, Y., Jiang, S., Wu, F., Zhou, Q., Shi, Z.L., Huang, J., 2022. Novel sarbecovirus bispecific neutralizing antibodies with exceptional breadth and potency against currently circulating SARS-CoV-2 variants and sarbecoviruses. *Cell Discov.* 8 (1), 36. <https://doi.org/10.1038/s41421-022-00401-6>.
- Wisniewski, J.R., Zougman, A., Nagaraj, N., Mann, M., 2009. Universal sample preparation method for proteome analysis. *Nat. Methods* 6 (5), 359–362. <https://doi.org/10.1038/nmeth.1322>.
- Yang, D., Su, M., Li, C., Zhang, B., Qi, S., Sun, D., Yin, B., 2020. Isolation and characterization of a variant subgroup GII-a porcine epidemic diarrhea virus strain in China. *Microb. Pathog.* 140, 103922 <https://doi.org/10.1016/j.micpath.2019.103922>.
- Yuan, X., Yao, Z., Wu, J., Zhou, Y., Shan, Y., Dong, B., Zhao, Z., Hua, P., Chen, J., Cong, Y., 2007. G1 phase cell cycle arrest induced by SARS-CoV 3a protein via the cyclin D3/pRb pathway. *Am. J. Respir. Cell Mol. Biol.* 37 (1), 9–19. <https://doi.org/10.1165/rcmb.2005-0345RC>.
- Zecha, J., Lee, C.Y., Bayer, F.P., Meng, C., Grass, V., Zerweck, J., Schnatbaum, K., Michler, T., Pichlmair, A., Ludwig, C., Kuster, B., 2020. Data, reagents, assays and merits of proteomics for SARS-CoV-2 research and testing. *Mol. Cell. Proteom.* 19 (9), 1503–1522. <https://doi.org/10.1074/mcp.RA120.002164>.
- Zheng, Z.Q., Wang, S.Y., Xu, Z.S., Fu, Y.Z., Wang, Y.Y., 2021. SARS-CoV-2 nucleocapsid protein impairs stress granule formation to promote viral replication. *Cell Discov.* 7 (1), 38. <https://doi.org/10.1038/s41421-021-00275-0>.